

Observation of $\bar{B}^0 \rightarrow D^{(*)0} p \bar{p}$

K. Abe,⁹ K. Abe,⁴² R. Abe,²⁹ T. Abe,⁴³ Byoung Sup Ahn,¹⁶ H. Aihara,⁴⁴ M. Akatsu,²² Y. Asano,⁴⁹ T. Aso,⁴⁸
 V. Aulchenko,² T. Aushev,¹³ A. M. Bakich,³⁹ Y. Ban,³³ E. Banas,²⁷ A. Bay,¹⁹ I. Bedny,² P. K. Behera,⁵⁰ A. Bondar,²
 A. Bozek,²⁷ M. Bračko,^{20,14} J. Brodzicka,²⁷ T. E. Browder,⁸ B. C. K. Casey,⁸ P. Chang,²⁶ Y. Chao,²⁶ B. G. Cheon,³⁸
 R. Chistov,¹³ S.-K. Choi,⁷ Y. Choi,³⁸ M. Danilov,¹³ L. Y. Dong,¹¹ J. Dragic,²¹ A. Drutskoy,¹³ S. Eidelman,² V. Eiges,¹³
 Y. Enari,²² F. Fang,⁸ C. Fukunaga,⁴⁶ N. Gabyshev,⁹ A. Garmash,^{2,9} T. Gershon,⁹ A. Gordon,²¹ R. Guo,²⁴ F. Handa,⁴³
 T. Hara,³¹ Y. Harada,²⁹ N. C. Hastings,²¹ H. Hayashii,²³ M. Hazumi,⁹ E. M. Heenan,²¹ I. Higuchi,⁴³ T. Higuchi,⁴⁴
 T. Hojo,³¹ T. Hokune,²² Y. Hoshi,⁴² K. Hoshina,⁴⁷ S. R. Hou,²⁶ W.-S. Hou,²⁶ S.-C. Hsu,²⁶ H.-C. Huang,²⁶ T. Igaki,²²
 Y. Igarashi,⁹ T. Iijima,²² K. Inami,²² A. Ishikawa,²² R. Itoh,⁹ H. Iwasaki,⁹ Y. Iwasaki,⁹ H. K. Jang,³⁷ J. Kaneko,⁴⁵
 J. H. Kang,⁵³ J. S. Kang,¹⁶ P. Kapusta,²⁷ N. Katayama,⁹ H. Kawai,³ Y. Kawakami,²² N. Kawamura,¹ T. Kawasaki,²⁹
 H. Kichimi,⁹ D. W. Kim,³⁸ Heejong Kim,⁵³ H. J. Kim,⁵³ H. O. Kim,³⁸ Hyunwoo Kim,¹⁶ S. K. Kim,³⁷ T. H. Kim,⁵³
 K. Kinoshita,⁵ S. Korpar,^{20,14} P. Krokovny,² R. Kulasiri,⁵ S. Kumar,³² A. Kuzmin,² Y.-J. Kwon,⁵³ J. S. Lange,^{6,35}
 G. Leder,¹² S. H. Lee,³⁷ J. Li,³⁶ D. Liventsev,¹³ R.-S. Lu,²⁶ J. MacNaughton,¹² G. Majumder,⁴⁰ F. Mandl,¹²
 S. Matsumoto,⁴ K. Miyabayashi,²³ H. Miyake,³¹ H. Miyata,²⁹ G. R. Moloney,²¹ T. Mori,⁴ T. Nagamine,⁴³ Y. Nagasaka,¹⁰
 T. Nakadaira,⁴⁴ E. Nakano,³⁰ M. Nakao,⁹ J. W. Nam,³⁸ Z. Natkaniec,²⁷ K. Neichi,⁴² S. Nishida,¹⁷ O. Nitoh,⁴⁷
 S. Noguchi,²³ T. Nozaki,⁹ S. Ogawa,⁴¹ F. Ohno,⁴⁵ T. Ohshima,²² T. Okabe,²² S. Okuno,¹⁵ S. L. Olsen,⁸ Y. Onuki,²⁹
 W. Ostrowicz,²⁷ H. Ozaki,⁹ P. Pakhlov,¹³ H. Palka,²⁷ C. W. Park,¹⁶ H. Park,¹⁸ K. S. Park,³⁸ L. S. Peak,³⁹ J.-P. Perroud,¹⁹
 M. Peters,⁸ L. E. Piiilonen,⁵¹ N. Root,² M. Rozanska,²⁷ K. Rybicki,²⁷ H. Sagawa,⁹ S. Saitoh,⁹ Y. Sakai,⁹ H. Sakamoto,¹⁷
 M. Satopathy,⁵⁰ A. Satopathy,^{9,5} O. Schneider,¹⁹ S. Schrenk,⁵ C. Schwanda,^{9,12} S. Semenov,¹³ K. Senyo,²² R. Seuster,⁸
 M. E. Sevir,²¹ H. Shibuya,⁴¹ B. Shwartz,² V. Sidorov,² J. B. Singh,³² S. Stanič,^{49,*} M. Starič,¹⁴ A. Sugi,²²
 A. Sugiyama,²² K. Sumisawa,⁹ T. Sumiyoshi,^{9,46} K. Suzuki,⁹ S. Suzuki,⁵² S. K. Swain,⁸ T. Takahashi,³⁰ F. Takasaki,⁹
 K. Tamai,⁹ N. Tamura,²⁹ M. Tanaka,⁹ G. N. Taylor,²¹ Y. Teramoto,³⁰ S. Tokuda,²² T. Tomura,⁴⁴ S. N. Tovey,²¹ K. Trabelsi,⁸
 T. Tsuboyama,⁹ T. Tsukamoto,⁹ S. Uehara,⁹ K. Ueno,²⁶ Y. Unno,³ S. Uno,⁹ S. E. Vahsen,³⁴ G. Varner,⁸ K. E. Varvell,³⁹
 C. C. Wang,²⁶ C. H. Wang,²⁵ J. G. Wang,⁵¹ M.-Z. Wang,²⁶ Y. Watanabe,⁴⁵ E. Won,¹⁶ B. D. Yabsley,⁵¹ Y. Yamada,⁹
 A. Yamaguchi,⁴³ Y. Yamashita,²⁸ M. Yamauchi,⁹ H. Yanai,²⁹ J. Yashima,⁹ Y. Yuan,¹¹ J. Zhang,⁴⁹ Z. P. Zhang,³⁶
 V. Zhilich,² and D. Žontar⁴⁹

(Belle Collaboration)

¹Aomori University, Aomori

²Budker Institute of Nuclear Physics, Novosibirsk

³Chiba University, Chiba

⁴Chuo University, Tokyo

⁵University of Cincinnati, Cincinnati, Ohio

⁶University of Frankfurt, Frankfurt

⁷Gyeongsang National University, Chinju

⁸University of Hawaii, Honolulu, Hawaii

⁹High Energy Accelerator Research Organization (KEK), Tsukuba

¹⁰Hiroshima Institute of Technology, Hiroshima

¹¹Institute of High Energy Physics, Chinese Academy of Sciences, Beijing

¹²Institute of High Energy Physics, Vienna

¹³Institute for Theoretical and Experimental Physics, Moscow

¹⁴J. Stefan Institute, Ljubljana

¹⁵Kanagawa University, Yokohama

¹⁶Korea University, Seoul

¹⁷Kyoto University, Kyoto

¹⁸Kyungpook National University, Taegu

¹⁹Institut de Physique des Hautes Énergies, Université de Lausanne, Lausanne

²⁰University of Maribor, Maribor

²¹University of Melbourne, Victoria

²²Nagoya University, Nagoya

²³Nara Women's University, Nagoya

²⁴National Kaohsiung Normal University, Kaohsiung

²⁵National Lien-Ho Institute of Technology, Miao Li

- ²⁶*National Taiwan University, Taipei*
²⁷*H. Niewodniczanski Institute of Nuclear Physics, Krakow*
²⁸*Nihon Dental College, Niigata*
²⁹*Niigata University, Niigata*
³⁰*Osaka City University, Osaka*
³¹*Osaka University, Osaka*
³²*Panjab University, Chandigarh*
³³*Peking University, Peking*
³⁴*Princeton University, Princeton, New Jersey*
³⁵*RIKEN BNL Research Center, Brookhaven, New York*
³⁶*University of Science and Technology of China, Hefei*
³⁷*Seoul National University, Seoul*
³⁸*Sungkyunkwan University, Suwon*
³⁹*University of Sydney, Sydney, New South Wales*
⁴⁰*Tata Institute of Fundamental Research, Bombay*
⁴¹*Toho University, Funabashi*
⁴²*Tohoku Gakuin University, Tagajo*
⁴³*Tohoku University, Sendai*
⁴⁴*University of Tokyo, Tokyo*
⁴⁵*Tokyo Institute of Technology, Tokyo*
⁴⁶*Tokyo Metropolitan University, Tokyo*
⁴⁷*Tokyo University of Agriculture and Technology, Tokyo*
⁴⁸*Toyama National College of Maritime Technology, Toyama*
⁴⁹*University of Tsukuba, Tsukuba*
⁵⁰*Utkal University, Bhubaneswer*
⁵¹*Virginia Polytechnic Institute and State University, Blacksburg, Virginia*
⁵²*Yokkaichi University, Yokkaichi*
⁵³*Yonsei University, Seoul*

(Received 24 May 2002; published 23 September 2002)

The B meson decay modes $B \rightarrow Dp\bar{p}$ and $B \rightarrow D^*p\bar{p}$ have been studied using 29.4 fb^{-1} of data collected with the Belle detector at KEKB. The $\bar{B}^0 \rightarrow D^0p\bar{p}$ and $\bar{B}^0 \rightarrow D^{*0}p\bar{p}$ decays have been observed for the first time with branching fractions $\mathcal{B}(\bar{B}^0 \rightarrow D^0p\bar{p}) = (1.18 \pm 0.15 \pm 0.16) \times 10^{-4}$ and $\mathcal{B}(\bar{B}^0 \rightarrow D^{*0}p\bar{p}) = (1.20_{-0.29}^{+0.33} \pm 0.21) \times 10^{-4}$. No signal has been found for the $B^+ \rightarrow D^+p\bar{p}$ and $B^+ \rightarrow D^{*+}p\bar{p}$ decay modes, and the corresponding upper limits at 90% C.L. are presented.

DOI: 10.1103/PhysRevLett.89.151802

PACS numbers: 13.25.Hw, 14.40.Nd

Until now, information on B decays with baryons in the final states is rather scarce. A recent search for the two-body baryonic B decays by Belle showed that their relative probabilities are rather small: for the decay modes $B^0 \rightarrow p\bar{p}, \Lambda\bar{\Lambda}$, and $B^+ \rightarrow p\bar{\Lambda}$ upper limits of $(1 - 2) \times 10^{-6}$ were obtained [1]. At the same time, measurements of the $B^0 \rightarrow D^{*-}p\bar{p}\pi^+$ and $B^0 \rightarrow D^{*-}p\bar{n}$ decay branching fractions by CLEO [2] and the observation of the $B^+ \rightarrow p\bar{p}K^+$ decay by Belle [3] indicate the dominance of multibody final states in decays of B mesons into baryons. Moreover, the observation of the $\bar{B}^0 \rightarrow D^0\pi^0$, $\bar{B}^0 \rightarrow D^0\eta$, and $\bar{B}^0 \rightarrow D^0\omega$ decays by Belle [4] and CLEO [5] with branching fractions considerably higher than expected indicates that color-suppressed B decays with baryons in the final state are likely to be sizable. This motivated a search for the color-suppressed decays $B \rightarrow D^{(*)}p\bar{p}$. The inclusion of charge conjugate modes is implicit throughout this report.

We use a data sample collected with the Belle detector at the KEKB asymmetric energy e^+e^- collider [6]. It consists of 29.4 fb^{-1} taken at the $\Upsilon(4S)$ resonance corresponding to $N_{B\bar{B}} = 31.9 \times 10^6$ produced $B\bar{B}$

pairs, and 2.3 fb^{-1} taken 60 MeV below the $\Upsilon(4S)$ resonance to perform systematic studies of the $e^+e^- \rightarrow q\bar{q}$ background.

The Belle detector [7] is a large-solid-angle magnetic spectrometer that consists of a three-layer silicon vertex detector, a 50-layer central drift chamber (CDC) for charged particle tracking and specific ionization measurement (dE/dx), an array of aerogel threshold Čerenkov counters (ACC), time-of-flight scintillation counters (TOF), and a CsI(Tl) electromagnetic calorimeter located in the magnetic volume. The magnetic field is returned via an iron yoke that is instrumented to detect muons and K_L mesons.

Charged tracks are selected with requirements based on the average hit residual and impact parameter relative to the interaction point. We also require that the transverse momentum of the tracks be greater than $0.1 \text{ GeV}/c$ to reduce the low momentum combinatorial background.

For particle identification (PID), the combined information from CDC, TOF, and ACC subsystems is used. Protons and antiprotons are selected with a set of PID criteria that has an efficiency of 98% and a kaon misidentification probability of 15%. Selection criteria for

charged kaons provide an efficiency of 88%, a pion misidentification probability of 8%, and negligible contamination from protons. All tracks positively identified as electrons are rejected.

A pair of calorimeter showers with an invariant mass within 15 MeV/c² of the nominal π^0 mass is considered as a π^0 candidate. An energy of at least 50 MeV and a photonlike shape are required for each shower.

We reconstruct D mesons in the following decay channels: $D^0 \rightarrow K^- \pi^+$, $D^0 \rightarrow K^- \pi^+ \pi^+ \pi^-$, $D^0 \rightarrow K^- \pi^+ \pi^0$, and $D^+ \rightarrow K^- \pi^+ \pi^+$. We select D candidates using cuts around the central values of the $M(D)$ distributions that correspond to 95% efficiency. For the π^0 from the $D^0 \rightarrow K^- \pi^+ \pi^0$ decay, we require that the π^0 momentum in the $Y(4S)$ center-of-mass (c.m.) frame be greater than 0.2 GeV/c in order to reduce combinatorial background. D^* mesons are reconstructed in the $D^{*0} \rightarrow D^0 \pi^0$ and $D^{*+} \rightarrow D^0 \pi^+$ decay modes. Since the pions from $D^* \rightarrow D\pi$ decays are slow, we relax these cuts and impose an energy threshold for π^0 photons of 30 MeV and a π^\pm transverse momentum threshold of 50 MeV/c. The mass difference between D^* and D candidates is required to be within 4 MeV from the expected value for D^{*0} and 2.5 MeV for D^{*+} ($\sim 3\sigma$ in both cases).

We combine $D^{(*)}$ candidates with $p\bar{p}$ pairs to form B mesons. Candidate events are identified by their c.m. energy difference, $\Delta E = (\sum_i E_i) - E_b$, and the beam constrained mass, $M_{bc} = \sqrt{E_b^2 - (\sum_i \vec{p}_i)^2}$, where E_b is the beam energy and \vec{p}_i and E_i are the momenta and energies of the decay products of the B meson in the c.m. frame. We select events with $M_{bc} > 5.20$ GeV/c² and $|\Delta E| < 0.2$ GeV, and define a B signal region of 5.272 GeV/c² $< M_{bc} < 5.288$ GeV/c² and $|\Delta E| < 0.020$ GeV. In the cases when there is more than one candidate in an event, the $B \rightarrow Dp\bar{p}$ (or $B \rightarrow D^*p\bar{p}$) candidate with the D mass (or $D^* - D$ mass difference) closest to the world average is chosen. We use Monte Carlo (MC) simulation with a three-body phase space distribution for the $B \rightarrow D^{(*)}p\bar{p}$ decays to model the response of the detector and determine the efficiency [8].

To suppress the large combinatorial background that is dominated by the two-jet-like $e^+e^- \rightarrow q\bar{q}$ continuum process, variables that characterize the event topology are used. We require $|\cos\theta_{\text{thr}}| < 0.80$, where θ_{thr} is the angle between the thrust axis of the B candidate and that of the rest of the event. This cut eliminates 77% of the continuum background and retains 78% of the signal events. We also define a Fisher discriminant, \mathcal{F} , which includes the production angle of the B candidate, the angle of the B candidate thrust axis with respect to the beam axis, and nine parameters that characterize the momentum flow in the event relative to the B candidate thrust axis in the c.m. frame [9]. We impose a requirement on \mathcal{F} that rejects 28% of the remaining continuum background and retains 95% of the signal.

The ΔE distributions were fitted with a Gaussian for the signal and a linear function for the background. The Gaussian mean value and width were fixed from the MC simulation of the signal events. In the fit to the ΔE distribution, the region $\Delta E < -0.1$ GeV is excluded to avoid contributions from other B decays, such as $B \rightarrow D^{(*)}\pi p\bar{p}$. For the calculation of branching fractions, we use the signal yields determined from the fit to the ΔE distribution. This minimizes a possible bias from other B meson decays, which tend to peak in M_{bc} but not in ΔE .

The ΔE distributions for the $\bar{B}^0 \rightarrow D^0 p\bar{p}$ and $\bar{B}^0 \rightarrow D^{*0} p\bar{p}$ decays are shown in Figs. 1 and 2. The fit results are presented in Table I, where the efficiency errors include only MC statistics. The significance quoted in Table I is defined as $\sqrt{-2 \ln(\mathcal{L}_0/\mathcal{L}_{\text{max}})}$, where \mathcal{L}_{max} and \mathcal{L}_0 denote the maximum likelihood with the nominal signal yield and with signal yield fixed at zero, respectively. Statistically, significant signals are observed for the $\bar{B}^0 \rightarrow D^0 p\bar{p}$ decay mode in all three decay channels of the D^0 meson. The corresponding branching fractions are in good agreement with each other. For the final result, we use a simultaneous fit to the three D^0 decay channels. The ΔE distributions for each mode were fitted together by a sum of a signal Gaussian and linear background function taking into account the corresponding detection efficiencies and D^0 meson branching fractions. The normalization of the background was allowed to float while the signal yields were required to

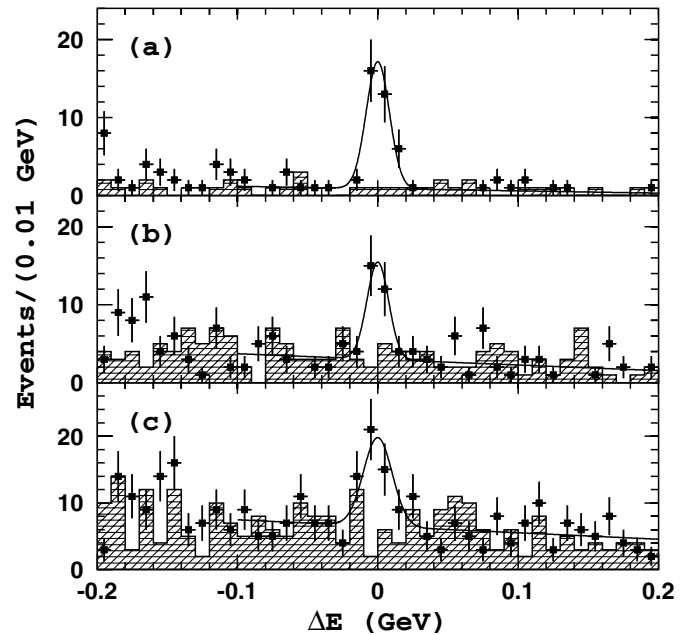


FIG. 1. The ΔE distributions for the $\bar{B}^0 \rightarrow D^0 p\bar{p}$ candidates: (a) $D^0 \rightarrow K^- \pi^+$, (b) $D^0 \rightarrow K^- \pi^+ \pi^+ \pi^-$, and (c) $D^0 \rightarrow K^- \pi^+ \pi^0$. The points with errors are experimental data, the hatched histograms are D^0 mass sidebands, and the curves are fit results.

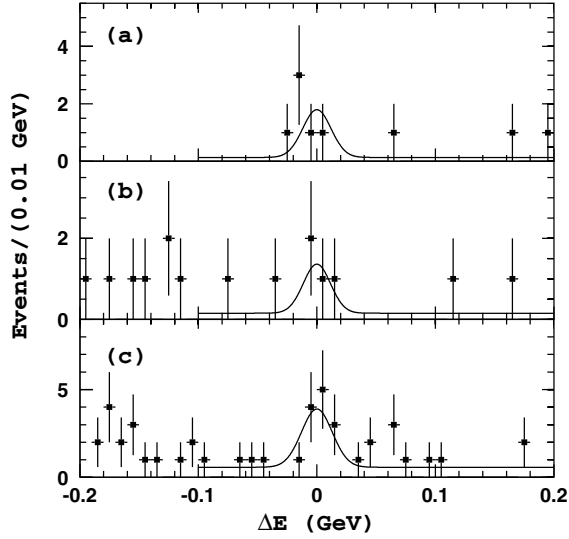


FIG. 2. The ΔE distributions for the $\bar{B}^0 \rightarrow D^{*0} p \bar{p}$ candidates: (a) $D^0 \rightarrow K^- \pi^+$, (b) $D^0 \rightarrow K^- \pi^+ \pi^+ \pi^-$, and (c) $D^0 \rightarrow K^- \pi^+ \pi^0$. The points with errors are experimental data and the curves are fit results.

satisfy the constraint: $N_i = N_{B\bar{B}} \mathcal{B}(\bar{B}^0 \rightarrow D^0 p \bar{p}) \mathcal{B}(D^0 \rightarrow X_i) \epsilon_i$, where the branching fraction $\mathcal{B}(\bar{B}^0 \rightarrow D^0 p \bar{p})$ is a fit parameter; $N_{B\bar{B}}$ is the number of $B\bar{B}$ pairs [10], $\mathcal{B}(D^0 \rightarrow X_i)$ are the D^0 meson branching fractions to the final states and X_i and ϵ_i are the corresponding efficiencies.

The signals in the $\bar{B}^0 \rightarrow D^{*0} p \bar{p}$ decay mode are less prominent but, when combined, have a 5.6σ statistical significance. As a cross-check, we confirm that the distribution in the $-0.2 \text{ GeV} < \Delta E < -0.15 \text{ GeV}$ region of the $\bar{B}^0 \rightarrow D^0 p \bar{p}$ mode is consistent with background from $\bar{B}^0 \rightarrow D^{*0} p \bar{p}$ with this measured branching fraction.

The $B^+ \rightarrow D^+ p \bar{p}$ and $B^+ \rightarrow D^{*+} p \bar{p}$ decays are doubly Cabibbo-Kobayashi-Maskawa suppressed and,

thus, are expected to have much smaller branching fractions. This is confirmed by the analysis of the corresponding distributions: We do not observe any signal for the $B^+ \rightarrow D^+ p \bar{p}$ and $B^+ \rightarrow D^{*+} p \bar{p}$ decays and present for them upper limits at 90% confidence level (C.L.) The Feldman-Cousins procedure [11] was used to calculate upper limits except for the simultaneous fit, where the maximum likelihood method was applied. In this case, the upper limit N was calculated from the relation $\int_0^N \mathcal{L}(n) dn = 0.9 \int_0^\infty \mathcal{L}(n) dn$, where $\mathcal{L}(n)$ is the maximum likelihood with the signal yield at n . The systematic uncertainties were taken into account in these calculations.

Figure 3(a) shows the Dalitz plot for the $\bar{B}^0 \rightarrow D^0 p \bar{p}$ candidates from the B signal region. For comparison, also shown in Fig. 3(a) is the same distribution for MC $\bar{B}^0 \rightarrow D^0 p \bar{p}$ signal events generated according to phase space. It is worth noting that, apart from a threshold enhancement in the invariant mass of $p \bar{p}$ (and possibly also $D^0 p$), the main part of the signal is distributed according to phase space. The Dalitz plot for the $\bar{B}^0 \rightarrow D^{*0} p \bar{p}$ channel (not shown) with a smaller statistics also reveals a similar tendency.

Since the $p \bar{p}$ invariant mass distribution of the observed signal is not completely described by the phase space distribution and the detection efficiency can be non-uniform over the Dalitz plot, some systematic uncertainty in the efficiency calculations may occur. To study the model dependence of the branching fractions, we fit the ΔE distribution for $\bar{B}^0 \rightarrow D^0 p \bar{p}$ candidates in six bins of $p \bar{p}$ invariant mass and calculate the partial branching fraction separately for each bin. The results are presented in Fig. 3(b) and in Table II. Summing up the partial branching fraction for each bin, we obtain the total $\bar{B}^0 \rightarrow D^0 p \bar{p}$ branching fraction $\mathcal{B}(\bar{B}^0 \rightarrow D^0 p \bar{p}) = (1.12^{+0.16}_{-0.14} \pm 0.16) \times 10^{-4}$. We apply

TABLE I. Branching fractions and 90% C.L. upper limits for $B \rightarrow D^{(*)} p \bar{p}$ decays.

Mode	ΔE yield	M_{bc} yield	Efficiency, %	$\mathcal{B}, 10^{-4}$	Significance
$\bar{B}^0 \rightarrow D^0 p \bar{p}, D^0 \rightarrow K^- \pi^+$	$33.6^{+6.5}_{-5.8}$	$34.5^{+6.5}_{-5.8}$	23.56 ± 0.49	$1.17^{+0.23}_{-0.20} \pm 0.14$	8.9σ
$\bar{B}^0 \rightarrow D^0 p \bar{p}, D^0 \rightarrow K^- \pi^+ \pi^+ \pi^-$	$24.2^{+6.3}_{-5.7}$	$14.7^{+5.8}_{-5.1}$	7.11 ± 0.21	$1.42^{+0.37}_{-0.34} \pm 0.22$	5.6σ
$\bar{B}^0 \rightarrow D^0 p \bar{p}, D^0 \rightarrow K^- \pi^+ \pi^0$	$34.2^{+8.6}_{-7.9}$	$36.5^{+8.2}_{-7.4}$	7.28 ± 0.28	$1.06^{+0.27}_{-0.24} \pm 0.15$	5.1σ
$\bar{B}^0 \rightarrow D^0 p \bar{p}$, simultaneous fit	$1.18 \pm 0.15 \pm 0.16$	12σ
$\bar{B}^0 \rightarrow D^{*0} p \bar{p}, D^{*0} \rightarrow D^0 \pi^0, D^0 \rightarrow K^- \pi^+$	$5.0^{+2.8}_{-2.2}$	$6.1^{+2.9}_{-2.3}$	8.11 ± 0.30	$0.81^{+0.46}_{-0.36} \pm 0.13$	2.9σ
$\bar{B}^0 \rightarrow D^{*0} p \bar{p}, D^{*0} \rightarrow D^0 \pi^0, D^0 \rightarrow K^- \pi^+ \pi^+ \pi^-$	$3.5^{+2.4}_{-1.7}$	$2.6^{+2.4}_{-1.8}$	1.96 ± 0.15	$1.21^{+0.82}_{-0.59} \pm 0.23$	2.6σ
$\bar{B}^0 \rightarrow D^{*0} p \bar{p}, D^{*0} \rightarrow D^0 \pi^0, D^0 \rightarrow K^- \pi^+ \pi^0$	$10.8^{+4.0}_{-3.4}$	$13.6^{+4.4}_{-3.8}$	2.38 ± 0.16	$1.65^{+0.61}_{-0.52} \pm 0.30$	4.2σ
$\bar{B}^0 \rightarrow D^{*0} p \bar{p}$, simultaneous fit	$1.20^{+0.33}_{-0.29} \pm 0.21$	5.6σ
$B^+ \rightarrow D^+ p \bar{p}, D^+ \rightarrow K^- \pi^+ \pi^+$	<5.2	<5.1	14.28 ± 0.38	<0.15 90% C.L.	...
$B^+ \rightarrow D^{*+} p \bar{p}, D^{*+} \rightarrow D^0 \pi^+, D^0 \rightarrow K^- \pi^+$	<2.2	<2.3	9.55 ± 0.31	<0.34 90% C.L.	...
$B^+ \rightarrow D^{*+} p \bar{p}, D^{*+} \rightarrow D^0 \pi^+, D^0 \rightarrow K^- \pi^+ \pi^+ \pi^-$	<1.8	<2.4	2.54 ± 0.16	<0.53 90% C.L.	...
$B^+ \rightarrow D^{*+} p \bar{p}, D^{*+} \rightarrow D^0 \pi^+, D^0 \rightarrow K^- \pi^+ \pi^0$	<4.8	<6.2	3.18 ± 0.18	<0.61 90% C.L.	...
$B^+ \rightarrow D^{*+} p \bar{p}$, simultaneous fit	<0.15 90% C.L.	...

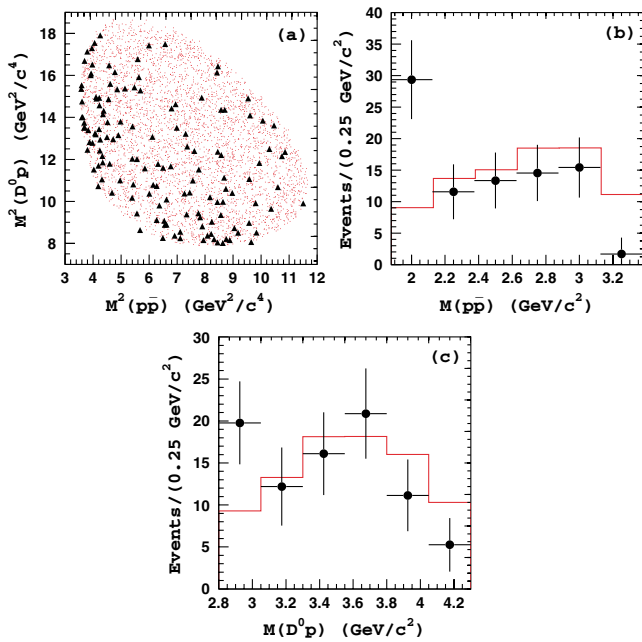


FIG. 3 (color online). (a) Dalitz plot for $\bar{B}^0 \rightarrow D^0 p \bar{p}$ candidates in the B signal region. The triangles show events in the data, and the small dots show the phase space simulation. The corresponding invariant mass spectra obtained by fitting the ΔE distribution in each bin are shown in (b) for $p \bar{p}$ and (c) for $D^0 p$, the data indicated by points and the phase space MC by histograms.

a similar procedure to the $D^0 p$ invariant mass. The results are presented in Fig. 3(c). In this case, the total $\bar{B}^0 \rightarrow D^0 p \bar{p}$ branching fraction is $\mathcal{B}(\bar{B}^0 \rightarrow D^0 p \bar{p}) = (1.11^{+0.16}_{-0.14} \pm 0.16) \times 10^{-4}$, consistent with the previous estimate. The difference with the result of the simultaneous fit presented in Table I is interpreted as a model-dependent error. The same model dependence is assumed for the $\bar{B}^0 \rightarrow D^{*0} p \bar{p}$ channel.

We examined the possibility that other B meson decay modes might produce backgrounds that peak in the signal region by means of a MC sample of generic $B\bar{B}$ events that corresponds to about 2.6 times the data statistics. No peaking backgrounds were found.

The following sources of systematic errors were found to be sizable: the tracking efficiency (2% per track), proton/antiproton identification efficiency (3% per particle), kaon identification efficiency (2%), π^0 efficiency (4%), efficiency for slow pions from $D^* \rightarrow D\pi$ decays (8% both for π^+ and π^0), $D^{(*)}$ branching fraction uncertainties (2%–6%), model-dependent error (5%), and MC statistics (3% for $B \rightarrow D p \bar{p}$, 6% for $B \rightarrow D^* p \bar{p}$). The tracking efficiency error was estimated using η decays to $\gamma\gamma$ and $\pi^+\pi^-\pi^0$. The proton identification uncertainty was determined from a sample of $\Lambda \rightarrow p\pi^-$ events; the error in kaon selection is obtained from $D^{*+} \rightarrow D^0\pi^+$, $D^0 \rightarrow K^-\pi^+$ decays. The π^0 reconstruction uncertainty was obtained using D^0 decays to $K^-\pi^+$ and $K^-\pi^+\pi^0$. The uncertainty in the ΔE signal shape parametrization

TABLE II. Branching fraction for the $\bar{B}^0 \rightarrow D^0 p \bar{p}$ in bins of the $p \bar{p}$ invariant mass.

$M(p\bar{p})$, GeV	ΔE yield	Efficiency, %	\mathcal{B} , 10^{-5}
<2.13	$29.4^{+6.6}_{-5.9}$	10.01 ± 0.44	$3.65^{+0.82}_{-0.73} \pm 0.51$
2.13–2.38	$11.6^{+4.7}_{-4.0}$	9.01 ± 0.32	$1.60^{+0.65}_{-0.55} \pm 0.22$
2.38–2.63	$13.4^{+4.8}_{-4.1}$	8.15 ± 0.28	$2.04^{+0.73}_{-0.61} \pm 0.29$
2.63–2.88	$14.5^{+4.8}_{-4.2}$	9.57 ± 0.30	$1.88^{+0.62}_{-0.54} \pm 0.26$
2.88–3.13	$15.4^{+5.1}_{-4.4}$	10.65 ± 0.34	$1.80^{+0.59}_{-0.51} \pm 0.25$
> 3.13	$1.7^{+2.6}_{-1.7}$	9.18 ± 0.37	$0.22^{+0.34}_{-0.22} \pm 0.03$
Total	$86.0^{+12.0}_{-10.4}$...	$11.2^{+1.6}_{-1.4} \pm 1.6$

(3%) was determined by varying the mean and width of the signal Gaussian within their errors. The combined systematic error is 14% for $\bar{B}^0 \rightarrow D^0 p \bar{p}$ ($B^+ \rightarrow D^+ p \bar{p}$) and 17% for $\bar{B}^0 \rightarrow D^{*0} p \bar{p}$ ($B^+ \rightarrow D^{*+} p \bar{p}$).

In summary, we report the first observation of the color-suppressed $\bar{B}^0 \rightarrow D^0 p \bar{p}$ and $\bar{B}^0 \rightarrow D^{*0} p \bar{p}$ decay modes. The measured branching fractions are $\mathcal{B}(\bar{B}^0 \rightarrow D^0 p \bar{p}) = (1.18 \pm 0.15 \pm 0.16) \times 10^{-4}$ and $\mathcal{B}(\bar{B}^0 \rightarrow D^{*0} p \bar{p}) = (1.20^{+0.33}_{-0.29} \pm 0.21) \times 10^{-4}$ with 12 σ and 5.6 σ statistical significance, respectively. No signal is observed in the $B^+ \rightarrow D^+ p \bar{p}$ and $B^+ \rightarrow D^{*+} p \bar{p}$ final states. The corresponding upper limits at 90% C.L. are $\mathcal{B}(B^+ \rightarrow D^+ p \bar{p}) < 0.15 \times 10^{-4}$ and $\mathcal{B}(B^+ \rightarrow D^{*+} p \bar{p}) < 0.15 \times 10^{-4}$.

We thank the KEKB accelerator group for the excellent operation of the KEKB accelerator. We acknowledge support from the Ministry of Education, Culture, Sports, Science, and Technology of Japan and the Japan Society for the Promotion of Science; the Australian Research Council and the Australian Department of Industry, Science and Resources; the National Science Foundation of China under Contract No. 10175071; the Department of Science and Technology of India; the BK21 program of the Ministry of Education of Korea and the CHEP SRC program of the Korea Science and Engineering Foundation; the Polish State Committee for Scientific Research under Contract No. 2P03B 17017; the Ministry of Science and Technology of the Russian Federation; the Ministry of Education, Science and Sport of the Republic of Slovenia; the National Science Council and the Ministry of Education of Taiwan; and the U.S. Department of Energy.

*On leave from Nova Gorica Polytechnic, Slovenia.

- [1] Belle Collaboration, K. Abe *et al.*, Phys. Rev. D **65**, 091103 (2002).
- [2] CLEO Collaboration, S. Anderson *et al.*, Phys. Rev. Lett. **86**, 2732 (2001).
- [3] Belle Collaboration, K. Abe *et al.*, Phys. Rev. Lett. **88**, 181803 (2002).

-
- [4] Belle Collaboration, K. Abe *et al.*, Phys. Rev. Lett. **88**, 052002 (2002).
- [5] CLEO Collaboration, T.E. Coan *et al.*, Phys. Rev. Lett. **88**, 062001 (2002).
- [6] KEKB Accelerator Papers, edited by E. Kikutani, KEK preprint 2001-157, Nucl. Instrum. Meth. A (to be published).
- [7] Belle Collaboration, A. Abashian *et al.*, Nucl. Instrum. Meth. A **479**, 117 (2002).
- [8] Events are generated with the CLEO group's QQ program; the detector response is simulated with GEANT, R. Brun *et al.* GEANT 3.21, CERN Report DD/EE/84-1, 1984.
- [9] CLEO Collaboration, D. M. Asner *et al.*, Phys. Rev. D **53**, 1039 (1996).
- [10] We assume that $N_{B^0\bar{B}^0} = N_{B^+B^-}$.
- [11] G. J. Feldman and R. D. Cousins, Phys. Rev. D **57**, 3873 (1998).